



Perspective

On the successes and opportunities for discovery of metal oxide photoanodes for solar fuels generators

Lan Zhou, Aniketa Shinde, Dan Guevarra, Joel A. Haber,
Kristin A. Persson, Jeffrey B. Neaton, and John M. Gregoire

ACS Energy Lett., **Just Accepted Manuscript** • Publication Date (Web): 31 Mar 2020

Downloaded from pubs.acs.org on March 31, 2020

Just Accepted

“Just Accepted” manuscripts have been peer-reviewed and accepted for publication. They are posted online prior to technical editing, formatting for publication and author proofing. The American Chemical Society provides “Just Accepted” as a service to the research community to expedite the dissemination of scientific material as soon as possible after acceptance. “Just Accepted” manuscripts appear in full in PDF format accompanied by an HTML abstract. “Just Accepted” manuscripts have been fully peer reviewed, but should not be considered the official version of record. They are citable by the Digital Object Identifier (DOI®). “Just Accepted” is an optional service offered to authors. Therefore, the “Just Accepted” Web site may not include all articles that will be published in the journal. After a manuscript is technically edited and formatted, it will be removed from the “Just Accepted” Web site and published as an ASAP article. Note that technical editing may introduce minor changes to the manuscript text and/or graphics which could affect content, and all legal disclaimers and ethical guidelines that apply to the journal pertain. ACS cannot be held responsible for errors or consequences arising from the use of information contained in these “Just Accepted” manuscripts.

On the successes and opportunities for discovery of metal oxide photoanodes for solar fuels generators

Lan Zhou,^a Aniketa Shinde,^a Dan Guevarra,^a Joel A. Haber,^a Kristin A. Persson,^{b,c,d} Jeffrey B. Neaton,^{b,e,f} John M. Gregoire^{a,g,}*

^a Joint Center for Artificial Photosynthesis, California Institute of Technology; Pasadena, California 91125, United States; ^b Joint Center for Artificial Photosynthesis, Lawrence Berkeley National Laboratory, Berkeley, CA 94720, United States; ^c Department of Materials Science and Engineering, University of California, Berkeley, CA 94720, United States; ^d Environmental Energy Technologies Division, Lawrence Berkeley National Laboratory; ^e Department of Physics, University of California, Berkeley, Berkeley, CA 94720, United States; ^f Molecular Foundry, Lawrence Berkeley National Laboratory, Berkeley, CA 94720, United States; Kavli Energy NanoSciences Institute, University of California, Berkeley, Berkeley, CA 94720, United States. ^g Division of Engineering and Applied Science, California Institute of Technology, Pasadena, CA 91125, United States

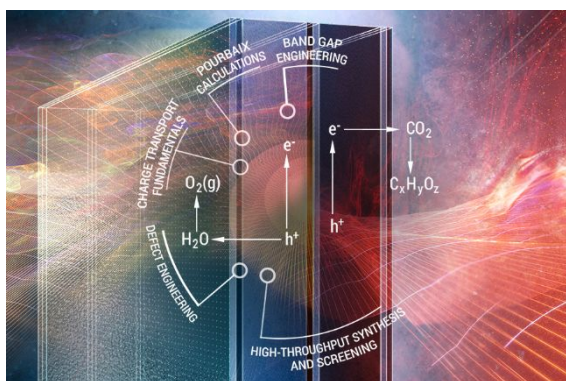
Corresponding Author

*gregoire@caltech.edu

ABSTRACT: The importance of metal oxide photoanodes in solar fuels technology has garnered concerted efforts in photoanode discovery in recent decades, which complement parallel efforts in

development of analytical techniques and optimization strategies using standard photoanodes such as TiO_2 , Fe_2O_3 and BiVO_4 . Theoretical guidance of high throughput experiments has been particularly effective in dramatically increasing the portfolio of metal oxide photoanodes, motivating a new era of photoanode development where the characterization and optimization techniques developed on traditional materials are applied to nascent photoanodes that exhibit visible light photoresponse. The compendium of metal oxide photoanodes presented in the present work can also serve as the basis for further technique development, with a primary goal to establish workflows for discovery of materials that perform better against the critical criteria of operational stability, visible light photoresponse, and photovoltage suitable for tandem absorber architectures.

TOC GRAPHICS



The generation of chemicals and fuels from CO_2 , N_2 , and H_2O in photoelectrochemical reactors would enable sustainable energy infrastructure with decreased reliance on photovoltaic and battery technologies that pose challenges for energy storage and transport.¹ The source chemical CO_2 is used for generation of C-containing chemicals such as CO and formate as well as higher-order fuels such as liquid hydrocarbons and alcohols that could displace fossil-based liquid fuels while leveraging existing infrastructure.² The source chemical N_2 is used for generation of NH_3 and less

1
2
3 often N_2H_4 , which may serve as fuels but can serve a more pressing need of sustainable fertilizer
4 production.³ These families of reactions involve electrochemical reduction of the source
5 chemicals, generally referred to as CO_2 reduction reactions (CO_2RR) and N_2 reduction reactions
6 (N_2RR), respectively. These reduction reactions require protons and electrons, and liberation of
7 those reactants from H_2O via the O_2 evolution reaction (OER) has been adopted as the primary
8 strategy for establishing broadly-deployable solar fuels technologies. The H_2 evolution reaction
9 (HER) can also be coupled to the OER without CO_2 or N_2 reactants, making solar
10 photoelectrocatalysis of the OER a cross-cutting technology for generation of H_2 , C-containing,
11 and N-containing fuels. Metal oxide photoanodes can also be used for anodic reactions other than
12 the OER, resulting in synthesis of other chemicals,⁴ although the present work considers solar fuels
13 photoanodes to be photoelectrocatalysts for the OER in aqueous electrolyte.

14
15 While photoelectrocatalysis of the HER and OER can occur with a single wide-gap
16 semiconductor, as demonstrated in the seminal water splitting work utilizing TiO_2 ,⁵ the broad
17 consensus, supported by multi-physics device modelling,⁶ is that efficient utilization of the solar
18 spectrum requires tandem light absorbers with band gap energies in the visible spectrum. While a
19 number of device architectures utilizing a pair of visible-gap semiconductors have been proposed,
20 a grand challenge of the solar fuels community has been the identification of a suitable solar fuels
21 photoanode, i.e. a semiconductor that can utilize visible light to effect photoelectrocatalysis of the
22 OER and circumvent a broad range of deactivation processes such as corrosion.

23
24 Photovoltaic-grade semiconductors, most notably III-V semiconductors, have enabled a variety
25 of high efficiency solar water splitting demonstrations.⁷ While protective coating⁸ of photovoltaic
26 semiconductors has been effective in increasing operational stability from minutes to over 100
27 hours,⁷ semiconductors that don't self-passivate under operational conditions will always be

1
2
3 susceptible to device failure upon damage in the protective coating(s). This type of single point
4 failure is difficult to circumvent in systems engineering and can render the technology untenable
5 for deployment. Intrinsic stability of the semiconductors is the most reliable way to achieve a
6 durable solar fuels generator, which has motivated the persistent and continuing effort to
7 understand metal oxide semiconductors and identify those that can serve as solar fuels
8 photoanodes. No fundamental limit on the efficiency of metal oxide photoanodes has been
9 established beyond those dictated by the thermodynamics of solar energy conversion, and BiVO₄-
10 based devices with ca. 5% efficiency are approaching these limits given its 2.4 eV band gap.⁹
11 Photoanode band gap energies no larger than 2 eV are required to realize the 15%-20% solar to
12 fuel conversion efficiencies, the target range per technoeconomic and device models,^{6, 10} requiring
13 the community to pursue a combination of low band gap energy and high radiative efficiency that
14 has yet to be approached by metal oxide photoanodes.
15
16
17
18
19
20
21
22
23
24
25
26
27
28
29

30 To establish the outlook for this grand challenge, we first summarize the progress to date. Recent
31 reviews have highlighted a broad portfolio of materials, techniques and devices. Abdi and
32 Berglund¹¹ recently reviewed metal oxide photoanodes with focus on the optimization of BiVO₄
33 and its implementation into water splitting devices, along with summary of several other V, W and
34 Fe-based oxide photoanodes, covering in total 9 metal oxide photoanode phases. Chu et al.¹²
35 focused more on classes of materials and the integration of photoelectrodes into devices. He et
36 al.¹³ compiled a more detailed survey of metal oxide photoanodes with 33 phases discussed and
37 critical analysis of several topics including the electronic character of the conduction and valence
38 bands and other electronic structure considerations. Our literature survey, summarized in Fig. 1
39 and detailed in the SI, identified 109 OER metal oxide photoanode phases, including recent
40 discoveries from our labs. Of these, we find 70 visible light-active phases, corresponding to
41
42
43
44
45
46
47
48
49
50
51
52
53
54
55
56
57
58
59
60

1
2
3 photoanodes demonstrated to be photoactive with only sub-3 eV illumination.[§] The breadth of
4
5 elements utilized in photoanode studies is rapidly expanding, and the number of visible light-active
6
7 metal oxide photoanodes has increased 5-fold in the past 20 years, an acceleration in discovery
8
9 driven by the concerted efforts in the community, including our high throughput discovery
10
11 program in the Joint Center for Artificial Photosynthesis (JCAP). During these 20 years, there has
12
13 also been substantial effort to develop and deploy the present champion visible-gap metal oxide
14
15 photoanode, BiVO₄.^{11, 14} These parallel community efforts in discovery of new metal oxide
16
17 photoanodes and in optimization and understanding of BiVO₄, both of which have been
18
19 remarkably successful, provide the framework for the future of the field.
20
21
22
23

24 BiVO₄ is an exemplar of a complex metal-oxide, visible-light photoanode whose study has
25
26 established the basis for accelerating development of metal oxide photoanodes.¹⁵ In addition to
27
28 optimization schemes such as defect engineering for charge transport and selective carrier
29
30 extraction,¹⁶ research on BiVO₄ has resulted in development of a broad range of materials and
31
32 device-level solar fuels characterization techniques.¹⁷ A recent review of strategies for enhancing
33
34 the photocurrent, photovoltage, and stability of photoelectrodes highlights the breadth and
35
36 effectiveness of feedback between synthesis and characterization of device-relevant parameters to
37
38 optimize materials, as illustrated in Fig. 2.¹⁷ The breadth of these materials development strategies
39
40 far exceeds the breadth of candidate photoanodes for which they have been deployed. The general
41
42 bias in scientific research towards continued investigation of well-researched materials is both
43
44 broadly known and recently evaluated as a limitation on creativity and discovery,¹⁸ motivating our
45
46 effort in the present work to establish the set of known visible light-active photoanodes and discuss
47
48 opportunities for improving performance both within this set of materials and beyond, via new
49
50 materials discovery strategies.
51
52
53
54
55
56
57
58
59
60

1
2
3 Of the 70 visible light-active metal oxide photoanodes, historically Fe_2O_3 and more recently
4 BiVO_4 are arguably the only materials for which the community has deeply invested in detailed
5 understanding and optimization, motivating further study on the other 68 phases, or some
6 principled selection of a subset thereof. Some notable efforts in this area include detailed
7 experimental investigation of $\alpha\text{-SnWO}_4$,¹⁹ Fe_2WO_6 ,²⁰ copper vanadates such as $\beta\text{-Cu}_2\text{V}_2\text{O}_7$ and $\gamma\text{-}$
8 $\text{Cu}_3\text{V}_2\text{O}_8$,²¹ and computational investigation of $\beta\text{-Cu}_2\text{V}_2\text{O}_7$ ²² to elucidate performance-limiting
9 properties. Of these, only the copper vanadates exhibit a photon energy onset of photoactivity near
10 2 eV, the desired upper-limit described above. Fig. 3 summarizes the photon energy onset for 49
11 metal oxide photoanodes that exhibit external quantum efficiency (EQE) in excess of 0.01% in our
12 experiments. Two notable phases with photoactivity at 2.1 eV (but insufficient to meet the EQE
13 threshold) are $\text{VCrO}_4\text{-orth}$ ²³ and $\text{V}_2\text{CoO}_6\text{-tri}$.²⁴ The 4 phases that exceed the threshold at 2.1 eV
14 are FeBiO_3 , discovered by Chen et al.,²⁵ as well as FeWO_4 ,²⁶ $\gamma\text{-V}_2\text{Cu}_3\text{O}_8$,²⁷ and $\text{Y}_3\text{Fe}_5\text{O}_{12}$,²⁴
15 highlighting the challenge of identifying metal oxide photoanodes with broad spectral response. A
16 chopped illumination voltage sweep is shown for each of these 4 phases, demonstrating that the
17 photocurrent decreases quickly with decreasing bias for most phases. Anecdotal examples
18 demonstrating improvement in operational photovoltage, i.e. beyond that exhibited in this figure,
19 include the observation of a turn on potential (lowest potential with observed photocurrent) near
20 0.6 V vs RHE for FeBiO_3 ²⁵ and near 0.4 V vs RHE for Bi-alloyed FeWO_4 .²⁶ More detailed
21 understanding of the semiconductor-liquid junctions and band energy alignment are needed to
22 elucidate the limiting photovoltage and associated efficiency of each photoanode, as discussed
23 further below.

24
25
26
27
28
29
30
31
32
33
34
35
36
37
38
39
40
41
42
43
44
45
46
47
48
49
50
51
52 With regards to the opportunity space for further discovery, it is interesting to consider the
53 fraction of the metal oxide search space that has been explored. The 70 visible light photoanodes
54
55
56
57
58
59
60

1
2
3 utilize 25 cation elements from the periodic table. Considering only ternary metal oxides, which
4 account for all but 6 of these phases, only 34 of the 300 pairwise combinations of these cations
5 have been reported. While some may have been explored without discovery, most remain
6 uncharted territory. High Throughput (HiTp) experimental screening of OER photoanodes,
7 pioneered by Parkinson²⁸ and McFarland²⁹ and advanced by others,³⁰ accelerates exploration of
8 this broad class of photoanode candidates, although the search space remains too large to be
9 comprehensively searched with brute force screening. Our research has, thus, focused on guidance
10 of high throughput experiments via theory-based identification of promising materials systems for
11 photoanode discovery.

12
13
14
15
16
17
18
19
20
21
22
23
24 The photoanodes identified by our high throughput screening (see SI) include 4 copper vanadates
25 that were identified simultaneously by HiTp theory and experiment.²³ These initial discoveries
26 motivated theory screening of Materials Project entries³¹ based on electronic structure and stability,
27 leading to experimental demonstration of photoanodic activity in 8 additional ternary metal
28 vanadates³² and 5 ternary metal manganates.²⁷ Experimental screening in composition spaces
29 related to these theory predictions resulted in the identification of an additional 29 photoanode
30 phases.^{24, 33} Perhaps the most important lesson from this work is that computational screening not
31 only identifies target phases but also promising composition regions that are sufficiently specific
32 to enable exploration by HiTp experiments, which are in turn sufficiently broad in scope to identify
33 materials beyond the computational search.

34
35
36
37
38
39
40
41
42
43
44
45
46
47 The fringe cases in these photoanode discovery campaigns offer insights for guiding future
48 discovery efforts. FeWO_4 was identified through combinatorial investigation of non-equilibrium
49 synthesis conditions.²⁶ This Fe^{+2} -containing metal oxide is stabilized against oxidation by a self-
50 passivation surface layer that includes Fe^{+3} , highlighting the role of self-passivation in enabling
51
52
53
54
55
56
57
58
59
60

1
2
3 stable operation of thermodynamically unstable photoanodes. Self-passivation was also observed
4
5 in copper vanadates, where the degradation in photocurrent was found to depend on the thickness
6
7 of the developed passivating film.³⁴ Passive surface films are of intense interest in the metals and
8
9 alloy industry and provide a fruitful research area in themselves as their formation and
10
11 functionality are still not entirely understood.³⁵ A range of phenomenological models have been
12
13 developed to explain the evolution of passivation layers, which display varying morphology, short-
14
15 range order and chemical constitution depending on the growth process and chemical
16
17 environment.³⁶ The stability of a passivating surface film, and hence that of the underlying bulk
18
19 material, is explicitly linked to ionic transport through the film which in turn depends critically on
20
21 the film morphology. Establishing thermodynamic and kinetic criteria for classifying a photoanode
22
23 as being operationally stable and supporting photoelectrocatalysis is a key area for designing the
24
25 next-generation of photoanode screening. In previous work,^{34, 37} we have found that well-
26
27 benchmarked Pourbaix diagrams³⁸ can provide a qualitative guide as to the likely formation of, as
28
29 well as general chemical composition of, a passive surface film. Furthermore, first-principles
30
31 methods have been shown to provide quantitative estimates for the relative Gibbs free energy and
32
33 corresponding aqueous regimes where a candidate photoanode material may form inert passivating
34
35 films, or steadily corrode to aqueous species.³⁷ Detailed understanding of the growth process,
36
37 evolution, and structure of these complex, self-passivation films is presently lacking, motivating
38
39 development of new computational and experimental techniques that lead to a predictive model
40
41 for how the near-surface of a given material will evolve under operational conditions.
42
43
44
45
46
47
48

49 The heterogeneous composition and structure of the photoanode as a function of depth from the
50
51 electrolyte surface complicates the already complex model of semiconductor-liquid junctions, as
52
53 the effect on these surface layers on band alignment and carrier transport have been insufficiently
54
55
56
57
58
59
60

1
2
3 studied to date. The standard thermodynamic requirement of band alignment, i.e. the vacuum
4 energy of the photoanode's valence band being sufficiently negative such that the photo-generated
5 holes are sufficiently oxidizing to drive the OER, is complicated by electrolyte pH-dependent
6 surface dipoles.³⁹ The polar surfaces of metal oxides introduce the additional complications of
7 facet and termination-dependent dipoles that alter this band alignment, as exemplified by
8 BiMn_2O_5 ⁴⁰ where band level calculations for each of 6 low-energy surfaces indicate more than 1.4
9 eV variation in work function, making the assessment of band alignment with respect to OER as
10 much of a property of the surface as it is of the bulk electronic structure. Further study of facet-
11 dependent and interfacial layer-dependent properties are likely to identify optimal photoanode
12 surfaces and guide synthesis and device implementation by designating desirable and undesirable
13 facets at the electrolyte interface. Initial demonstrations of this concept include facet-dependent
14 charge separation in BiVO_4 ⁴¹ and SrTiO_3 .⁴²

15
16
17
18
19
20
21
22
23
24
25
26
27
28
29
30
31 This aforementioned BiMn_2O_5 ,⁴⁰ as well as $\beta\text{-Mn}_2\text{V}_2\text{O}_7$,⁴³ provide additional opportunity to
32 investigate performance-limiting attributes of metal oxide photoanodes. The 1.8 eV direct gap of
33 each phase is ideal with respect to solar absorption, but they have yet to be demonstrated as OER
34 photoanodes. While operational stability is a prime suspect for a lack of photoactivity, these are
35 among the most electrochemically stable low-gap metal oxides, with Pourbaix-stable regions in
36 the approximate ranges 0.3-0.7 and 0.3-1.2 V vs RHE, respectively. Despite these desirable
37 attributes, these phases are not classified as photoanodes in the present work due to their
38 photoactivity only in the presence of sacrificial hole acceptors. The modest photoactivity obtained
39 with sacrificial hole acceptors also indicates that the photoanode performance limitations extend
40 beyond poor OER catalysis. From an electronic structure point of view, these are exemplary
41 photoanode candidates, motivating detailed inspection as to whether materials optimization can
42
43
44
45
46
47
48
49
50
51
52
53
54
55
56
57
58
59
60

1
2
3 confer higher photoactivity, and/or identification of fundamental properties that limit photoactivity
4
5 with commensurate design of associated screening techniques.
6

7
8 Ternary manganate phases also illustrate the challenges of treating high-temperature or
9
10 disordered magnetic states in electronic structure calculations. For these ternary manganates, zero-
11
12 temperature calculations with judiciously-chosen magnetic configurations were required to gauge
13
14 the possible electronic structure of each phase's ambient temperature paramagnetic state;^{40, 43}
15
16 paramagnetic states, in which the local magnetic moments on each open-shell cation are nonzero
17
18 but their configurational average is zero, are not trivially-compatible with periodic supercells.
19
20 Typically, high-throughput computational screening employs a computationally less expensive
21
22 model of the magnetic state, e.g. the ferromagnetic configuration, which can induce significant
23
24 changes to the electronic structure⁴⁴ of the material compared to the paramagnetic state. In our
25
26 experience, this approximation can lead to exclusion of promising low-gap metal oxides that
27
28 exhibit a metallic character in their ferromagnetic state. Antiferromagnetic (AF) ordering is
29
30 typically a better approximation of the paramagnetic state, and currently the Materials Project is
31
32 pursuing a large computational survey of the magnetic state of its materials including at least one
33
34 AF ordering for each transition metal oxide.⁴⁴ Other approaches for computational modelling of
35
36 paramagnetic materials have been introduced in the literature,⁴⁵ creating an opportunity to evaluate
37
38 the electronic structure of photoanode materials at relevant operating temperatures.
39
40
41
42
43

44
45 The compendium of photoanode phases described in the SI offers various opportunities for
46
47 identifying trends and descriptors for photoactivity. A seldom-discussed materials property that is
48
49 well characterized by our combinatorial experiments is cation off-stoichiometry of metal oxide
50
51 photoanodes. Fig. 4 shows the EQE under 3.2 eV illumination for 55 $A_{1-x}B_x$ oxide phases, where
52
53 B is taken to be the higher valent cation produced by the Materials Project oxidation state
54
55
56
57
58
59
60

1
2
3 interpreter, and each phase is plotted by the difference in x between XRF measurements of thin
4 film composition and that of the formula unit (FU). In addition to showing the considerable
5 variation in EQE over the collection of metal oxide photoanodes, the observation of appreciable
6 EQE at substantial composition deviations is quite striking. There are 5 phases with composition
7 deviation more than 0.18 from the composition of the prototype structure. With this level of
8 composition deviation, nanocrystalline secondary phases (not detected by XRD) may be present,
9 although such composition differences often occur with a multi-valent cation such that the host
10 structure can support substantial alloying. For example, the phases with an excess of the higher
11 valent cation include formal valences A^{+2} ($A = \text{Ca}$ or Mg) and either Mn^{+3} or Mn^{+4} , where excess
12 Mn appears to alloy as Mn^{+2} on the A^{+2} site. There are also cases where the structure of interest is
13 only observed in off-stoichiometric conditions, such as $\text{V}_2\text{Ag}_{0.33}\text{O}_5$ where an excess of Ag is
14 needed to form the structure under our synthesis conditions, likely resulting in some metallic Ag
15 in the thin film sample. This level of off-stoichiometry in solar energy conversion materials has
16 been most extensively studied with Cu-based p-type semiconductors such as $\text{Cu}(\text{In},\text{Ga})\text{Se}_2$,⁴⁶
17 $\text{Cu}_2\text{SnZnS}_4$,⁴⁷ and CuBi_2O_4 ⁴⁸ where alloyed variants improve phase stability with respect to
18 competing phases and/or alter the electronic structure. These phenomena underlie the composition
19 variations of photoanodes in Fig. 4, where alloying can additionally optimize a catalytic activity
20 and/or electrochemical passivation.
21
22
23
24
25
26
27
28
29
30
31
32
33
34
35
36
37
38
39
40
41
42
43

44 The uncertainty in the XRF compositions is nominally 5 at.%, so phases appearing outside the
45 ± 0.06 window are confidently off-stoichiometric, bringing into question whether traditional
46 methods would discover these photoanodes. Of the 23 such phases, 7 are also photoactive within
47 the ± 0.06 window, so discovery may have been possible with synthesis at a composition matching
48 the target FU. The remaining 16 phases required composition deviation to be discovered in our
49
50
51
52
53
54
55
56
57
58
59
60

1
2
3 experiments, highlighting the utility of composition libraries in photoanode discovery and
4
5 motivating further study of how substantial alloying optimizes photoanode performance.
6

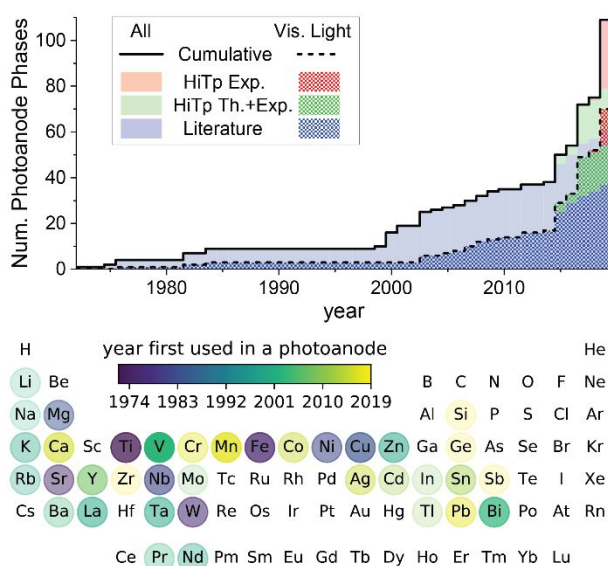
7
8 Intertwined with the cation off-stoichiometry is the oxygen stoichiometry, or oxygen vacancy
9
10 concentration, which is not amenable to high throughput characterization, resulting in a lack of
11
12 observable trends over the set of known photoanodes. Recent work on BiVO_4 has demonstrated
13
14 that over various time scales, the sub-band-gap states created by oxygen vacancies trap holes and
15
16 electrons, ultimately requiring thermal de-trapping to produce photoactivity.⁴⁹ These results
17
18 highlight the complexity of carrier transport in metal oxide photoanodes, which often involves
19
20 small polaron hopping⁵⁰ and may additionally involve more complex phenomena over a range of
21
22 time scales. An opportunity arising from these recent advances is determination of the extent to
23
24 which the observed conduction mechanisms of BiVO_4 are universal to ternary vanadates and other
25
26 metal oxide photoanodes, and if the electronic structure contributions of oxygen vacancies, for
27
28 example, can be used as a functional descriptor of metal oxide photoanodes. Our HiTp screening
29
30 work includes a concerted exploration of ternary vanadates where we demonstrated tuning of band
31
32 gap energies across the visible range through band edge hybridization with various open-d-shell
33
34 cations.²³ These are specific examples of a general property of metal oxide photoanodes: nontrivial
35
36 orbital character (particularly d orbital character) at band edges creates opportunities for tuning the
37
38 band-edge electronic structure in new ways, potentially leading to electron and hole conductivities
39
40 that are not well described by semi-classical, Boltzmann-based band transport theory.
41
42
43
44
45

46
47 Traditional semiconductor characterization of conductivity or effective carrier mobility is
48
49 necessary but insufficient for specific identification of the transport-limiting phenomenon. Recent
50
51 developments in ultrafast spectroscopy have demonstrated direct observation of polaron
52
53 formation,⁵¹ and application of such techniques to a broader class of photoanodes will help
54
55
56
57
58
59
60

1
2
3 establish trends in the roles of defects, excited states, etc. in metal oxide semiconductor transport.
4
5 Disentangling the transport mechanisms can also be facilitated by theory, although the highly-
6
7 localized and strongly correlated electronic states (e.g. states with d orbital character) typically
8
9 require rigorous treatment beyond that of standard theories and computational methods. Metal
10
11 oxides often exhibit such electronic states, and as noted above, photoanodes of interest often
12
13 encompass additional structural and chemical complexity that may alter transport properties and
14
15 may require treatment of many-atom systems, creating substantial computational expense.
16
17 Although DFT calculations are often used to compute band structures in practice, rigorous
18
19 calculations of spectroscopic properties of metal oxide photoanode candidates require formalisms
20
21 beyond the ground-state, time-independent DFT. In materials physics, the formalism of choice for
22
23 quantitative prediction of the band structure and optical properties is *ab initio* many-body
24
25 perturbation theory (MBPT).⁵² MBPT has been historically computationally prohibitive for
26
27 complex materials, but it is beginning to be applied to complex systems, such as the metal oxide
28
29 photoanodes BiVO₄ and β -Cu₂V₂O₇,^{22, 53} and interfaces involving photoanode materials and
30
31 water.⁵⁴ Additionally, detailed *ab initio* calculations of photoexcited carrier dynamics, limited by
32
33 phonon scattering, are now possible for simple semiconductors,⁵⁵ and have more recently been
34
35 extended to oxides.⁵⁶ A growing number of recent methodologies are being proposed for more
36
37 rigorous calculations of polaron formation energies.⁵⁷ Collectively, advances in these methods
38
39 promise a significantly deeper and richer understanding and assessment of photogenerated carrier
40
41 phenomena in existing candidate photoanodes, which will also lead to new descriptors for
42
43 discovery of photoelectrode materials.
44
45
46
47
48
49

50
51 Solar fuels photoanodes pose substantial challenges for materials discovery due to the combined
52
53 needs of solar absorption, charge carrier separation and transport, chemical and electrochemical
54
55
56
57
58
59
60

1
2
3 stability under operating conditions, as well as catalytic activity for the OER. The recent increase
4
5 in chemical diversity of metal oxide photoanodes presents both challenges, for example
6
7 determining which phases are amenable to optimization and integration into solar fuels generators,
8
9 and opportunities, for example developing new theory and experiment campaigns to better
10
11 understand fundamental properties that give rise to photoanodic activity. Despite the prolific
12
13 photoanode discovery efforts of the last 20 years, solar fuels photoanodes are still rare compared
14
15 to other types of functional materials, motivating continued identification of such materials to
16
17 formulate models that relate fundamental materials properties to photoanode performance,
18
19 enhancing scientific understanding as well as development of deployable solar fuels materials. The
20
21 photoactivity of off-stoichiometric variants of phases is notable, motivating application of defect
22
23 and transport characterization techniques, which have been recently developed via study of Fe_2O_3
24
25 and BiVO_4 , to a broader set of metal oxide phases. Combining the recent proliferation of both
26
27 photoanode discoveries and advanced characterization techniques will advance fundamental
28
29 understanding of metal oxide photoelectrocatalysts and the design of next-generation photoanodes.
30
31
32
33
34



35
36
37
38
39
40
41
42
43
44
45
46
47
48
49
50
51
52
53 Figure 1: (top) Summary of OER photoanodes from literature (blue), as well as our previous
54
55 reports integrating HiTp theory and experiment (green) and additional HiTp experiment
56
57
58
59
60

discoveries (red). (bottom) Using all photoanodes, the year in which each element was first used in a photoanode is shown on the periodic table, with the saturation of each circle corresponding to the number of times the element appears in the list of 109 photoanodes.

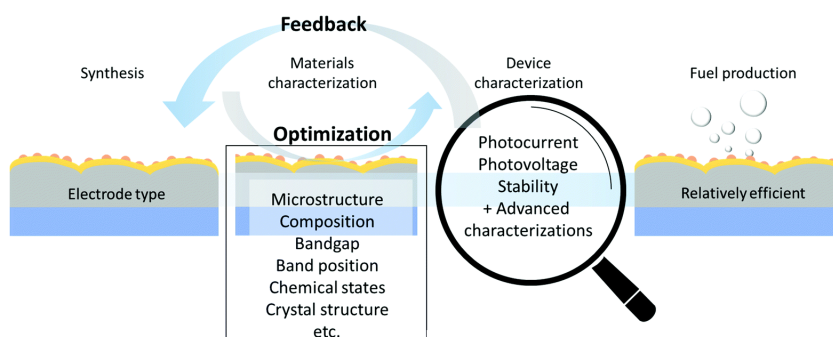


Figure 2: Illustration of synthesis and processing-based optimization of a library of materials properties, with feedback provided by an ever-expanding suite of materials and device-level characterizations. Adapted from Ref. ¹⁷ with permission.

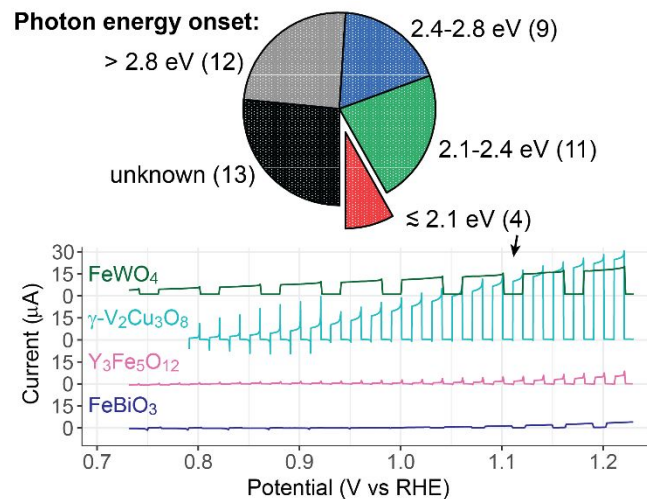


Figure 3: The pie chart shows the distribution of photon energy onset for photoactivity, for 49 metal oxide photoanode phases from combinatorial libraries with EQE in excess of 0.01% (see SI). The photon energy onset is determined via photoelectrochemistry at 1.23 V vs RHE with a

series of light emitting diodes, and due to their spectral breadth the boundaries between the 4 ranges have ca. ± 0.1 eV uncertainty. For the 4 photoanodes with photoactivity at 2.1 eV, the cathodic sweep from a cyclic voltammogram is shown with toggled 3.2 eV illumination (variable illumination intensity, see SI). These data were acquired in pH 13 (0.1 M NaOH) for γ - $V_2Cu_3O_8$ and $Y_3Fe_5O_{12}$ and borate-buffered pH 9.3 electrolyte for $FeWO_4$ and $FeBiO_3$, as reported previously.^{24, 26-27}

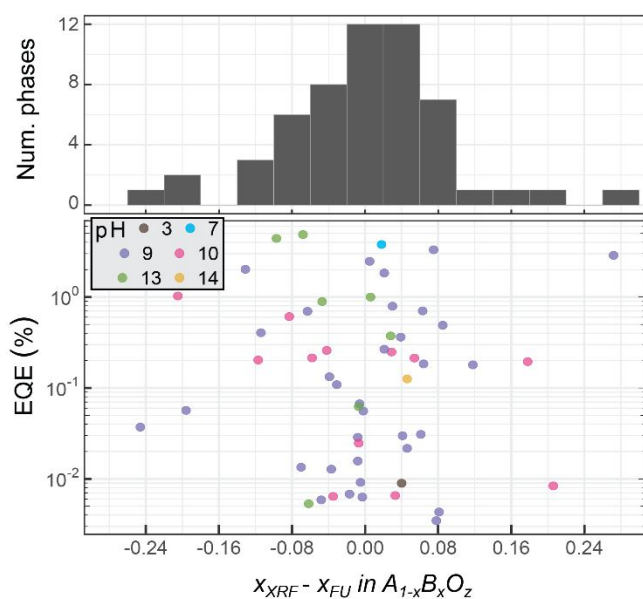


Figure 4: Summary of 55 photoanode phases from combinatorial libraries with available XRF measurement of composition. For each identified ternary oxide, the cation stoichiometry x is taken as $A_{1-x}B_xO_z$ where B is generally the higher valent cation. The quantity $x_{XRF} - x_{FU}$ is the difference in x between the composition of the most photoactive sample and that of the formula unit. The EQE at 3.2 eV is shown as the metric for photoactivity as this is the only illumination source used for all photoanode samples.

ASSOCIATED CONTENT

1
2
3 **Supporting Information.** Table of 109 metal oxide photoanodes from the literature survey
4 summarized in Fig. 1. Table of HiTp composition and photoelectrochemical data for 58 phases
5
6 measured in our labs.
7
8
9

10
11 **AUTHOR INFORMATION**
12

13
14 *gregoire@caltech.edu
15
16

17 **Notes**
18

19
20 The authors declare no competing financial interest.
21
22

23 § In the literature survey, photoactivity under white light illumination combined with optical
24 identification of a sub-2.8 eV band gap was considered to be sufficient evidence for a visible
25
26 light photoanode.
27
28
29

30
31 **AUTHOR BIOGRAPHIES**
32

33 Lan Zhou earned her Ph.D in Materials Science from University of Vermont in 2010, and is
34 currently working as a Staff Scientist in the High Throughput Experimentation group at Caltech.
35
36 Her research focuses on developing processes for combinatorial materials synthesis of metals,
37
38 metal oxides, and mixed anion materials used in solar-fuels applications.
39
40
41

42
43 Aniketa Shinde specializes in instrumentation, materials science, and electrochemistry for energy
44 research. Her focus is high-throughput scanning drop sensor measurements for
45
46 photoelectrochemical and electrochemical characterization of thin films. She received her Master's
47
48 and PhD degrees in Physics from the University of California, Irvine.
49
50
51

52
53 Dan Guevarra has been a member of the High Throughput Experimentation group and the Joint
54
55 Center for Artificial Photosynthesis at Caltech since 2013. He received a Master of Information
56
57
58
59
60

1
2
3 and Data Science from the University of California, Berkeley and presently works on data analysis,
4
5 visualization, machine learning, and instrument automation.
6
7

8
9 Joel A. Haber is a Staff Scientist at the California Institute of Technology in the Joint Center for
10
11 Artificial Photosynthesis. His research focuses on inorganic materials chemistry and high-
12
13 throughput materials science, as applied to materials and devices for solar-energy conversion.
14
15

16
17 Kristin A. Persson is an Associate Professor in Materials Science and Engineering at UC Berkeley
18
19 with a joint appointment as Senior Faculty Scientist at the Lawrence Berkeley National
20
21 Laboratory. She is also the Director of the Materials Project (www.materialsproject.org) and
22
23 specializes in materials informatics and data-driven design of novel materials.
24
25

26
27 Jeffrey B. Neaton is a Professor of Physics at UC Berkeley, and Senior Faculty Scientist and
28
29 Associate Laboratory Director for Energy Sciences at Lawrence Berkeley National Laboratory.
30
31 He is also a member of the Kavli Energy Nanosciences Institute at Berkeley. His research focuses
32
33 on the development and application of electronic structure theory for predictive calculations of
34
35 properties of inorganic and organic energy and quantum materials.
36
37

38
39 John Gregoire is the Thrust Coordinator for Photoelectrocatalysis in the Joint Center for Artificial
40
41 Photosynthesis, a U.S. DOE Energy Innovation Hub. He leads the High Throughput
42
43 Experimentation group at Caltech, which accelerates scientific discovery by automating critical
44
45 components of materials research workflows, from synthesis to data interpretation.
46
47
48
49
50

51
52 **ACKNOWLEDGMENT**
53
54
55
56
57
58
59
60

1
2
3 This material is based upon work performed by the Joint Center for Artificial Photosynthesis, a
4
5 DOE Energy Innovation Hub, supported through the Office of Science of the U.S. Department of
6
7 Energy under Award Number DE-SC0004993.
8
9

10 QUOTES TO HIGHLIGHT

11
12
13 Theoretical guidance of high throughput experiments has been particularly effective in
14 dramatically increasing the portfolio of metal oxide photoanodes, motivating a new era of
15 photoanode development where the characterization and optimization techniques developed on
16 traditional materials are applied to nascent photoanodes that exhibit visible light photoresponse.
17
18

19 Computational screening not only identifies target phases but also promising composition
20 regions that are sufficiently specific to enable exploration by high throughput experiments,
21 which are in turn sufficiently broad in scope to identify materials beyond the computational
22 search.
23

24 The photoactivity of off-stoichiometric variants of phases is notable, motivating application of
25 defect and transport characterization techniques, which have been recently developed via study
26 of Fe₂O₃ and BiVO₄, to a broader set of metal oxide phases.
27
28

29 Combining the recent proliferation of both photoanode discoveries and advanced
30 characterization techniques will advance fundamental understanding of metal oxide
31 photoelectrocatalysts and the design of next-generation photoanodes.
32
33

34 REFERENCES

- 35
36
37 1. Kraan, O.; Kramer, G. J.; Haigh, M.; Laurens, C., An Energy Transition That Relies Only
38 on Technology Leads to a Bet on Solar Fuels. *Joule* **2019**, *3* (10), 2286-2290.
39
40 2. Raciti, D.; Wang, C., Recent Advances in CO₂ Reduction Electrocatalysis on Copper.
41 *ACS Energy Letters* **2018**, *3* (7), 1545-1556.
42
43 3. Chen, X.; Li, N.; Kong, Z.; Ong, W.-J.; Zhao, X., Photocatalytic fixation of nitrogen to
44 ammonia: state-of-the-art advancements and future prospects. *Materials Horizons* **2018**, *5* (1), 9-
45 27.
46
47 4. Sayama, K., Production of High-Value-Added Chemicals on Oxide Semiconductor
48 Photoanodes under Visible Light for Solar Chemical-Conversion Processes. *ACS Energy Letters*
49 **2018**, *3* (5), 1093-1101.
50
51 5. Mavroides, J. G.; Tchernev, D. I.; Kafalas, J. A.; Kolesar, D. F., Photoelectrolysis of
52 water in cells with TiO₂ anodes. *Materials Research Bulletin* **1975**, *10* (10), 1023-1030.
53
54 6. Fountaine, K. T.; Lewerenz, H. J.; Atwater, H. A., Efficiency Limits for
55 Photoelectrochemical Water-Splitting. *Nat. Commun.* **2016**, *7*, 13706.
56
57 7. Tournet, J.; Lee, Y.; Karuturi, S. K.; Tan, H. H.; Jagadish, C., III–V Semiconductor
58 Materials for Solar Hydrogen Production: Status and Prospects. *ACS Energy Letters* **2020**, 611-
59 622.
60

8. Bae, D.; Seger, B.; Vesborg, P. C. K.; Hansen, O.; Chorkendorff, I., Strategies for stable water splitting via protected photoelectrodes. *Chem Soc Rev* **2017**, *46* (7), 1933-1954.
9. Kim, J. H.; Han, S.; Jo, Y. H.; Bak, Y.; Lee, J. S., A precious metal-free solar water splitting cell with a bifunctional cobalt phosphide electrocatalyst and doubly promoted bismuth vanadate photoanode. *Journal of Materials Chemistry A* **2018**, *6* (3), 1266-1274.
10. Sathre, R.; Greenblatt, J. B.; Walczak, K.; Sharp, I. D.; Stevens, J. C.; Ager, J. W.; Houle, F. A., Opportunities to improve the net energy performance of photoelectrochemical water-splitting technology. *Energ Environ Sci* **2016**, *9* (3), 803-819.
11. Abdi, F. F.; Berglund, S. P., Recent developments in complex metal oxide photoelectrodes. *Journal of Physics D: Applied Physics* **2017**, *50* (19), 193002.
12. Chu, S.; Li, W.; Yan, Y.; Hamann, T.; Shih, I.; Wang, D.; Mi, Z., Roadmap on solar water splitting: current status and future prospects. *Nano Futures* **2017**, *1* (2), 022001.
13. He, H.; Liao, A.; Guo, W.; Luo, W.; Zhou, Y.; Zou, Z., State-of-the-art progress in the use of ternary metal oxides as photoelectrode materials for water splitting and organic synthesis. *Nano Today* **2019**, 100763.
14. (a) Sayama, K.; Nomura, A.; Zou, Z. G.; Abe, R.; Abe, Y.; Arakawa, H., Photoelectrochemical Decomposition of Water on Nanocrystalline BiVO₄ Film Electrodes Under Visible Light. *Chem. Commun.* **2003**, (23), 2908-2909; (b) Lamm, B.; Trześniewski, B. J.; Döscher, H.; Smith, W. A.; Stefik, M., Emerging Postsynthetic Improvements of BiVO₄ Photoanodes for Solar Water Splitting. *ACS Energy Letters* **2018**, *3* (1), 112-124; (c) Kim, J. H.; Lee, J. S., Elaborately Modified BiVO₄ Photoanodes for Solar Water Splitting. *Advanced Materials* **2019**, *31* (20), 1806938.
15. Sharp, I. D.; Cooper, J. K.; Toma, F. M.; Buonsanti, R., Bismuth Vanadate as a Platform for Accelerating Discovery and Development of Complex Transition-Metal Oxide Photoanodes. *ACS Energy Letters* **2017**, *2* (1), 139-150.
16. Zhang, W.; Liu, M., Modulating Carrier Transport via Defect Engineering in Solar Water Splitting Devices. *ACS Energy Letters* **2019**, *4* (4), 834-843.
17. Yang, W.; Prabhakar, R. R.; Tan, J.; Tilley, S. D.; Moon, J., Strategies for enhancing the photocurrent, photovoltage, and stability of photoelectrodes for photoelectrochemical water splitting. *Chem Soc Rev* **2019**, *48* (19), 4979-5015.
18. Jia, X.; Lynch, A.; Huang, Y.; Danielson, M.; Lang'at, I.; Milder, A.; Ruby, A. E.; Wang, H.; Friedler, S. A.; Norquist, A. J.; Schrier, J., Anthropogenic biases in chemical reaction data hinder exploratory inorganic synthesis. *Nature* **2019**, *573* (7773), 251-255.
19. Kölbach, M.; Pereira, I. J.; Harbauer, K.; Plate, P.; Höflich, K.; Berglund, S. P.; Friedrich, D.; van de Krol, R.; Abdi, F. F., Revealing the Performance-Limiting Factors in α -SnWO₄ Photoanodes for Solar Water Splitting. *Chem Mater* **2018**, *30* (22), 8322-8331.
20. Abdi, F. F.; Chemseddine, A.; Berglund, S. P.; van de Krol, R., Assessing the Suitability of Iron Tungstate (Fe₂WO₆) as a Photoelectrode Material for Water Oxidation. *The Journal of Physical Chemistry C* **2017**, *121* (1), 153-160.
21. Jiang, C.-M.; Segev, G.; Hess, L. H.; Liu, G.; Zaborski, G.; Toma, F. M.; Cooper, J. K.; Sharp, I. D., Composition-Dependent Functionality of Copper Vanadate Photoanodes. *ACS Applied Materials & Interfaces* **2018**, *10* (13), 10627-10633.
22. Wiktor, J.; Reshetnyak, I.; Strach, M.; Scarongella, M.; Buonsanti, R.; Pasquarello, A., Sizable Excitonic Effects Undermining the Photocatalytic Efficiency of β -Cu₂V₂O₇. *The Journal of Physical Chemistry Letters* **2018**, *9* (19), 5698-5703.

- 1
2
3 23. Yan, Q.; Yu, J.; Suram, S. K.; Zhou, L.; Shinde, A.; Newhouse, P. F.; Chen, W.; Li, G.;
4 Persson, K. A.; Gregoire, J. M.; Neaton, J. B., Solar fuels photoanode materials discovery by
5 integrating high-throughput theory and experiment. *Proceedings of the National Academy of*
6 *Sciences of the United States of America* **2017**, *114* (12), 3040-3043.
- 7
8 24. Zhou, L.; Shinde, A.; Guevarra, D.; Richter, M. H.; Stein, H. S.; Wang, Y.; Newhouse,
9 P.; Persson, K.; Gregoire, J., Combinatorial screening yields discovery of 29 metal oxide
10 photoanodes for solar fuel generation. *Journal of Materials Chemistry A* **2020**,
11 10.1039/C9TA13829C.
- 12
13 25. Chen, X. Y.; Yu, T.; Gao, F.; Zhang, H. T.; Liu, L. F.; Wang, Y. M.; Li, Z. S.; Zou, Z.
14 G.; Liu, J. M., Application of weak ferromagnetic BiFeO₃ films as the photoelectrode material
15 under visible-light irradiation. *Appl. Phys. Lett.* **2007**, *91* (2).
- 16
17 26. Zhou, L.; Shinde, A.; Suram, S. K.; Stein, H. S.; Bauers, S. R.; Zakutayev, A.; DuChene,
18 J. S.; Liu, G.; Peterson, E. A.; Neaton, J. B.; Gregoire, J. M., Bi-Containing n-FeWO₄ Thin
19 Films Provide the Largest Photovoltage and Highest Stability for a Sub-2 eV Band Gap
20 Photoanode. *ACS Energy Letters* **2018**, *3* (11), 2769-2774.
- 21
22 27. Zhou, L.; Yan, Q.; Shinde, A.; Guevarra, D.; Newhouse, P. F.; Becerra-Stasiewicz, N.;
23 Chatman, S. M.; Haber, J. A.; Neaton, J. B.; Gregoire, J. M., High Throughput Discovery of
24 Solar Fuels Photoanodes in the CuO–V₂O₅ System. *Adv. Energy Mater.* **2015**, *5*, 1500968.
- 25
26 28. (a) Woodhouse, M.; Herman, G. S.; Parkinson, B. A., Combinatorial Approach to
27 Identification of Catalysts for the Photoelectrolysis of Water. *Chem. Mater.* **2005**, *17* (17), 4318-
28 4324; (b) Rowley, J. G.; Do, T. D.; Cleary, D. A.; Parkinson, B. A., Combinatorial Discovery
29 Through a Distributed Outreach Program: Investigation of the Photoelectrolysis Activity of p-
30 Type Fe, Cr, Al Oxides. *ACS Applied Materials & Interfaces* **2014**, *6* (12), 9046-9052.
- 31
32 29. Jaramillo, T. F.; Baeck, S. H.; Kleiman-Shwarsstein, A.; Choi, K. S.; Stucky, G. D.;
33 McFarland, E. W., Automated electrochemical synthesis and photoelectrochemical
34 characterization of Zn_{1-x}Co_xO thin films for solar hydrogen production. *J. Comb. Chem.* **2005**, *7*
35 (2), 264-271.
- 36
37 30. (a) Gutkowski, R.; Khare, C.; Conzuelo, F.; Kayran, Y. U.; Ludwig, A.; Schuhmann, W.,
38 Unraveling compositional effects on the light-induced oxygen evolution in Bi(V-Mo-X)O₄
39 material libraries. *Energ Environ Sci* **2017**, *10* (5), 1213-1221; (b) Meyer, R.; Sliozberg, K.;
40 Khare, C.; Schuhmann, W.; Ludwig, A., High-Throughput Screening of Thin-Film
41 Semiconductor Material Libraries II: Characterization of Fe-W-O Libraries. *ChemSusChem*
42 **2015**, *8* (7), 1279-1285; (c) Lee, J. W.; Ye, H. C.; Pan, S. L.; Bard, A. J., Screening of
43 photocatalysts by scanning electrochemical microscopy. *Anal. Chem.* **2008**, *80* (19), 7445-7450.
- 44
45 31. Jain, A.; Ong, S. P.; Hautier, G.; Chen, W.; Richards, W. D.; Dacek, S.; Cholia, S.;
46 Gunter, D.; Skinner, D.; Ceder, G.; Persson, K. A., The Materials Project: A materials genome
47 approach to accelerating materials innovation. *APL Materials* **2013**, *1* (1), 011002.
- 48
49 32. Shinde, A.; Suram, S. K.; Yan, Q.; Zhou, L.; Singh, A. K.; Yu, J.; Persson, K. A.;
50 Neaton, J. B.; Gregoire, J. M., Discovery of Manganese-Based Solar Fuel Photoanodes via
51 Integration of Electronic Structure Calculations, Pourbaix Stability Modeling, and High-
52 Throughput Experiments. *ACS Energy Letters* **2017**, 2307-2312.
- 53
54 33. Noh, J.; Kim, S.; Gu, G. h.; Shinde, A.; Zhou, L.; Gregoire, J. M.; Jung, Y., Unveiling
55 new stable manganese based photoanode materials via theoretical high-throughput screening and
56 experiments. *Chemical Communications* **2019**, 55, 13418-13421.
- 57
58 34. Zhou, L.; Yan, Q.; Yu, J.; Jones, R. J. R.; Becerra-Stasiewicz, N.; Suram, S. K.; Shinde,
59 A.; Guevarra, D.; Neaton, J. B.; Persson, K. A.; Gregoire, J. M., Stability and Self-passivation of
60

- Copper Vanadate Photoanodes under Chemical, Electrochemical, and Photoelectrochemical Operation. *Phys. Chem. Chem. Phys.* **2016**, *18*, 9349-9352.
35. (a) Macdonald, D. D., On the Existence of Our Metals-Based Civilization: I. Phase-Space Analysis. *Journal of The Electrochemical Society* **2006**, *153* (7), B213-B224; (b) Macdonald, D. D., Passivity—the key to our metals-based civilization. *Pure and Applied Chemistry* **1999**, *71* (6), 951-978.
36. (a) Macdonald, D. D.; Urquidi-Macdonald, M., Theory of Steady-State Passive Films. *Journal of The Electrochemical Society* **1990**, *137* (8), 2395-2402; (b) Schultze, J. W.; Lohrengel, M. M., Stability, reactivity and breakdown of passive films. Problems of recent and future research. *Electrochim Acta* **2000**, *45* (15), 2499-2513.
37. Singh, A. K.; Zhou, L.; Shinde, A.; Suram, S. K.; Montoya, J. H.; Winston, D.; Gregoire, J. M.; Persson, K. A., Electrochemical Stability of Metastable Materials. *Chem Mater* **2017**, *29* (23), 10159-10167.
38. Persson, K. A.; Waldwick, B.; Lazic, P.; Ceder, G., Prediction of solid-aqueous equilibria: Scheme to combine first-principles calculations of solids with experimental aqueous states. *Phys. Rev. B* **2012**, *85* (23), 235438.
39. Stevanovic, V.; Lany, S.; Ginley, D. S.; Tumas, W.; Zunger, A., Assessing capability of semiconductors to split water using ionization potentials and electron affinities only. *Phys Chem Chem Phys* **2014**, *16* (8), 3706-3714.
40. Newhouse, P. F.; Reyes-Lillo, S. E.; Li, G.; Zhou, L.; Shinde, A.; Guevarra, D.; Suram, S. K.; Soedarmadji, E.; Richter, M. H.; Qu, X.; Persson, K.; Neaton, J. B.; Gregoire, J. M., Discovery and Characterization of a Pourbaix-Stable, 1.8 eV Direct Gap Bismuth Manganate Photoanode. *Chem Mater* **2017**, *29* (23), 10027-10036.
41. Li, R.; Han, H.; Zhang, F.; Wang, D.; Li, C., Highly efficient photocatalysts constructed by rational assembly of dual-cocatalysts separately on different facets of BiVO₄. *Energ Environ Sci* **2014**, *7* (4), 1369-1376.
42. Mu, L.; Zhao, Y.; Li, A.; Wang, S.; Wang, Z.; Yang, J.; Wang, Y.; Liu, T.; Chen, R.; Zhu, J.; Fan, F.; Li, R.; Li, C., Enhancing charge separation on high symmetry SrTiO₃ exposed with anisotropic facets for photocatalytic water splitting. *Energ Environ Sci* **2016**, *9* (7), 2463-2469.
43. Yan, Q.; Li, G.; Newhouse, P. F.; Yu, J.; Persson, K. A.; Gregoire, J. M.; Neaton, J. B., Mn₂V₂O₇: An Earth Abundant Light Absorber for Solar Water Splitting. *Advanced Energy Materials* **2015**, *5* (8), 1401840.
44. Horton, M. K.; Montoya, J. H.; Liu, M.; Persson, K. A., High-throughput prediction of the ground-state collinear magnetic order of inorganic materials using Density Functional Theory. *npj Computational Materials* **2019**, *5* (1), 64.
45. (a) Mozafari, E.; Alling, B.; Steneteg, P.; Abrikosov, I. A., Role of N defects in paramagnetic CrN at finite temperatures from first principles. *Physical Review B* **2015**, *91* (9), 094101; (b) Abrikosov, I. A.; Ponomareva, A. V.; Steneteg, P.; Barannikova, S. A.; Alling, B., Recent progress in simulations of the paramagnetic state of magnetic materials. *Current Opinion in Solid State and Materials Science* **2016**, *20* (2), 85-106; (c) Trimarchi, G.; Wang, Z.; Zunger, A., Polymorphous band structure model of gapping in the antiferromagnetic and paramagnetic phases of the Mott insulators MnO, FeO, CoO, and NiO. *Physical Review B* **2018**, *97* (3), 035107.
46. Ramanujam, J.; Singh, U. P., Copper indium gallium selenide based solar cells – a review. *Energy & Environmental Science* **2017**, *10* (6), 1306-1319.

- 1
2
3 47. Dhawale, D. S.; Ali, A.; Lokhande, A. C., Impact of various dopant elements on the
4 properties of kesterite compounds for solar cell applications: a status review. *Sustainable Energy*
5 *& Fuels* **2019**, *3* (6), 1365-1383.
- 6 48. Sharma, G.; Zhao, Z.; Sarker, P.; Nail, B. A.; Wang, J.; Huda, M. N.; Osterloh, F. E.,
7 Electronic structure, photovoltage, and photocatalytic hydrogen evolution with p-CuBi₂O₄
8 nanocrystals. *Journal of Materials Chemistry A* **2016**, *4* (8), 2936-2942.
- 9 49. Selim, S.; Pastor, E.; García-Tecedor, M.; Morris, M. R.; Francàs, L.; Sachs, M.; Moss,
10 B.; Corby, S.; Mesa, C. A.; Gimenez, S.; Kafizas, A.; Bakulin, A. A.; Durrant, J. R., Impact of
11 Oxygen Vacancy Occupancy on Charge Carrier Dynamics in BiVO₄ Photoanodes. *Journal of*
12 *the American Chemical Society* **2019**, *141* (47), 18791-18798.
- 13 50. Rettie, A. J. E.; Chemelewski, W. D.; Emin, D.; Mullins, C. B., Unravelling Small-
14 Polaron Transport in Metal Oxide Photoelectrodes. *The Journal of Physical Chemistry Letters*
15 **2016**, *7* (3), 471-479.
- 16 51. Carneiro, L. M.; Cushing, S. K.; Liu, C.; Su, Y.; Yang, P.; Alivisatos, A. P.; Leone, S. R.,
17 Excitation-wavelength-dependent small polaron trapping of photoexcited carriers in α -Fe₂O₃.
18 *Nature Materials* **2017**, *16* (8), 819-825.
- 19 52. (a) Strinati, G., Application of the Green's functions method to the study of the optical
20 properties of semiconductors. *La Rivista del Nuovo Cimento (1978-1999)* **1988**, *11* (12), 1-86;
21 (b) Onida, G.; Reining, L.; Rubio, A., Electronic excitations: density-functional versus many-
22 body Green's-function approaches. *Reviews of Modern Physics* **2002**, *74* (2), 601-659; (c) Golze,
23 D.; Dvorak, M.; Rinke, P., The GW Compendium: A Practical Guide to Theoretical
24 Photoemission Spectroscopy. *Frontiers in Chemistry* **2019**, *7*, 377.
- 25 53. Wiktor, J.; Reshetnyak, I.; Ambrosio, F.; Pasquarello, A., Comprehensive modeling of
26 the band gap and absorption spectrum of BiVO₄. *Physical Review Materials* **2017**, *1* (2),
27 022401.
- 28 54. (a) Ambrosio, F.; Wiktor, J.; Pasquarello, A., pH-Dependent Catalytic Reaction Pathway
29 for Water Splitting at the BiVO₄-Water Interface from the Band Alignment. *ACS Energy Letters*
30 **2018**, *3* (4), 829-834; (b) Gerosa, M.; Gygi, F.; Govoni, M.; Galli, G., The role of defects and
31 excess surface charges at finite temperature for optimizing oxide photoabsorbers. *Nature*
32 *Materials* **2018**, *17* (12), 1122-1127.
- 33 55. (a) Bernardi, M.; Vigil-Fowler, D.; Lischner, J.; Neaton, J. B.; Louie, S. G., Ab Initio
34 Study of Hot Carriers in the First Picosecond after Sunlight Absorption in Silicon. *Physical*
35 *Review Letters* **2014**, *112* (25), 257402; (b) Bernardi, M.; Vigil-Fowler, D.; Ong, C. S.; Neaton,
36 J. B.; Louie, S. G., Ab initio study of hot electrons in GaAs. *Proceedings of the National*
37 *Academy of Sciences* **2015**, *112* (17), 5291-5296.
- 38 56. (a) Zhou, J.-J.; Hellman, O.; Bernardi, M., Electron-Phonon Scattering in the Presence of
39 Soft Modes and Electron Mobility in SrTiO₃ Perovskite from First Principles. *Physical Review*
40 *Letters* **2018**, *121* (22), 226603; (b) Zhou, J.-J.; Bernardi, M., Predicting charge transport in the
41 presence of polarons: The beyond-quasiparticle regime in SrTiO₃. *Physical Review Research*
42 **2019**, *1* (3), 033138.
- 43 57. Sio, W. H.; Verdi, C.; Poncé, S.; Giustino, F., Polarons from First Principles, without
44 Supercells. *Physical Review Letters* **2019**, *122* (24), 246403.
- 45
46
47
48
49
50
51
52
53
54
55
56
57
58
59
60